

Shooting Control Application from a Quadruped Robot with a Weapon System via Sliding-mode Control Method

Ahmet Burak Tatar^{#,*}, Alper Kadir Tanyıldızı[#], and Oğuz Yakut[#]

[#]Department of Mechatronics Engineering, Firat University, Elazig, Turkey

^{*}E-mail: atatar@firat.edu.tr

ABSTRACT

With the developing technological process, it is expected that the usage of robots will increase in defense systems as in every field. One of the main objectives of the robotic studies for the defense industry is to capture the targeted success under all kinds of disruptive effects with robotic systems and to present this technology to the service of the army. A weapon system with a single degree of freedom was placed on a quadruped robot. System's dynamic behavior, which has 12 degrees of freedom and planar movements, is modeled mathematically. Simulations of the shots made to the fixed targets were carried out during the walking of the quadruped robot. The gun barrel stabilization was realized to achieve accurate shots under disruptive effects. The sliding-mode control method was used to perform the barrel stabilisation. In this study, it is shown that a quadruped robot with a weapon system can perform successful shots against fixed targets. MATLAB is used for simulations and the results are shown with figures, graphics, and tables.

Keywords: Sliding-mode control; Target shooting; Barrel stabilisation; Quadruped robot

NOMENCLATURE

M	Robot body's mass	V_b	Bullet velocity
x	Robot body's position on horizontal axis	P_b	Repulsion pressure
y	Robot body's position on vertical axis	A_b	Pressure surface area
m_{1-8}	Robot leg limbs' masses	C_d	Friction coefficient between air and bullet
θ	Angular position to ground by vertical axis of Robot body	x_{target}	Target position on horizontal axis
θ_{1-8}	Angular positions of Leg limbs	y_{target}	Target position on vertical axis
l_g	Robot body's length	e_x	Horizontal position error
l_{1-8}	Length of Leg limb	e_y	Vertical position error
a	Length of gun turret	y_i	Foot-end's position on vertical axis
b	Length of gun barrel		
x_{1-8}	Robot leg limbs' positions on horizontal axis		
y_{1-8}	Robot leg limbs' positions on vertical axis		
I	Robot body's Inertia Moment		
α	Gun barrel's relative angular position to body		
x_n	Gun barrel's position on horizontal axis		
y_n	Gun barrel's position on vertical axis		
m_n	Gun barrel's mass		
β	Barrel reference angle		
g	Gravity		
h_{step}	Leg's height from the ground		
w	Step motion frequency		
L_s	Step length		
F_{thrust}	Bullet force		
F_{aero}	The surface frictional force of gravity and atmosphere		

1. INTRODUCTION

Significant advances have been made in military technology throughout human history and the history of wars, which has caused serious changes in military conflicts. With this process, one of the enemy's desire to reach superior weapon systems than the other is a critical point¹. In general, the basic definition and functional expectations of robotic and autonomous systems, which are defined as 'intelligent agents', are not very new. A machine concept that can artificially imitate people's movements, decisions, and behaviours have been part of a common culture for nearly 100 years². Weapon systems, which are used during the war, must be operational and should be able to work in environments where they are under disruptive effects³.

By adapting technological advances to the defense industry, new generation weapons are being developed today. The main purpose of these weapon systems is to ensure that, despite any disruptive effect, the target is successfully hit. In addition, weapon systems are preferred in combat conditions,

which are more mobile and react faster. Military advantage has always been aided by the capacity to inflict damage from a distance.⁴Here, the problem that needs to be overcome, is to reduce the error value between the target and the bullet. For this reason, the shooting control must be adjusted⁵. No matter how effective the destructive power is in moving weapon systems, the most critical efficiency factor is the stability of the gun barrel. For gun barrel stabilisation, the effectiveness of the shootings made on the mobile vehicle is also possible in these weapon systems. The shooting efficiency for the tanks is measured in today's technology, as with similar weapon systems, not only by shooting while the tank is stationary but also in motion. To shoot the target while it was in motion, the gun barrel was stabilised. The stabilisation system ensures gun barrel's angular position remains constant regardless of the position of the vehicle. In other words, the operator's intervention in the non-stabilised system is required to maintain the gun barrel's angular position relative to the ground. In the stabilised system, with the help of the control algorithm there is no need to require such an intervention. Thus, it is easier to track target⁶. The basis for stabilising the gun barrel is to control the angle of movement of the gun turret system. The ability to control the gun turret in a combat vehicle is critically important for the development of defence industry technology. The control of a two-axis gun turret system is ensured by the proper operation of azimuth and elevation angles to compensate for the distortions caused by the movement of the vehicle⁷.

Robotics technology made a serious improvement especially in the field of joint-legged robots, which has contributed to the world's defence industry. Compared to most wheeled and tracked robots, leg biomimetic robots can easily pass through rough terrain. Depending on the specification, legged robots can have one, two, four, six, or more legs. Among these are the most widely used quadruped robots in this field. The leg mechanism has a high DoF, real-time feedback, and large working space in the process of movement⁸.

A weapon system has been mounted on the quadruped robot and a planar model has been developed in this study and the results are presented graphically. The main purpose of the study is to transmit the oscillations with the PID controller during the trot walking as a disruptive effect to the gun barrel system and to stabilize the barrel with the sliding mode controller (SMC). It is thus aimed at hitting the fixed targets whose positions are determined randomly during walking with successful shots.

To examine the dynamic behaviour of the robot's walking motion, a walking pattern must be determined. Trot walking was used in this system. From some studies, it has been used to prefer trot walking⁹⁻¹⁰.

The sliding mode control method is one of the active control methods. One of its main advantages is that the sliding mode control is insensitive to external influences and parametric changes¹¹.

Rahmat¹², *et al.* used the SMC control method in their two degrees of freedom gun turret for target tracking. They concluded that the SMC controller has achieved high precision

and accuracy in tracking the target. Therefore, it has been effective in using the SMC control method in our system that these and similar studies in the literature for gun barrel stabilisation

To demonstrate the performance of the stabilisation of the gun barrel, randomly selected fixed targets were positioned in the range of 5-15 m opposite the robot. In Fig. 1, an image is given from the simulation of the shots made by a quadruped robot to fixed targets. The hitting success of these shots is given as a table in the study. During the shooting, mathematical expressions representing planar dynamic behaviour and ballistic of the projectile core were used in the simulations.

Throughout the simulation, β_{target} (target angle) was auto-updated and simultaneously calculated, taking into account the variable robot's position towards fixed targets while walking. The gun barrel reference angle can also be called the angle of elevation. The barrel reference angle is calculated using the right triangle hypotenuse, depending on the horizontal and vertical axis position error to the target. Simulations were carried out using the method of the numerical approach developed in MATLAB by Runge-Kutta.

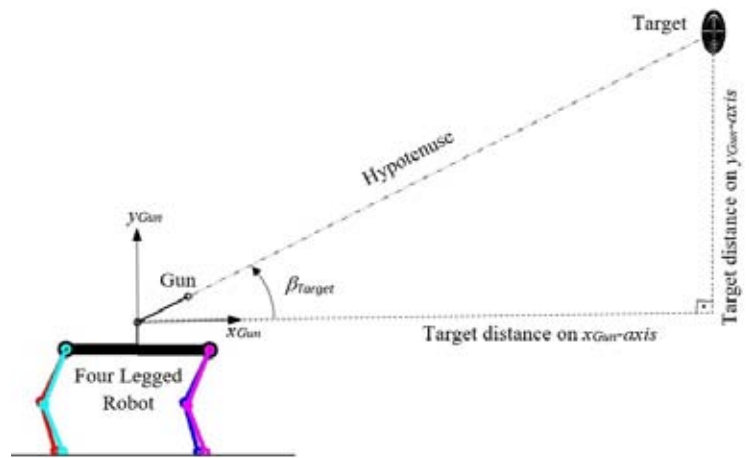


Figure 1. Shooting from the quadruped robot to fixed targets.

2. MATHEMATICAL MODEL

Figure 2 shows a physical model expressing the planar movement of a quadruped robot on which a uniaxial weapon system is placed. It is assumed that each leg has 2 DOFs and rotating joints in the robot's physical model. The system has a total of 12 degrees of freedom.

Mathematical equations of the planar motion of the robot are obtained. For this, the Euler-Lagrange method was used. Mathematical equations of the planar motion of the robot are obtained. For this, the Euler-Lagrange method was used. Euler-Lagrange (EL) systems represent a crucial dynamical system, for which the motions' equations can be derived via the EL equation¹³. To obtain the equations of the moving joints, the main expression of the Lagrange method was used as in Eqn. (1).

$$\frac{d}{dt} \frac{\partial}{\partial \dot{q}_i} L(q, \dot{q}_i) - \frac{\partial}{\partial q_i} L(q, \dot{q}_i) = \tau_i \quad 1 \leq i \leq n \quad (1)$$

here is the degree of freedom, q_i is the position of the moving joints, i shows the moving joints index.

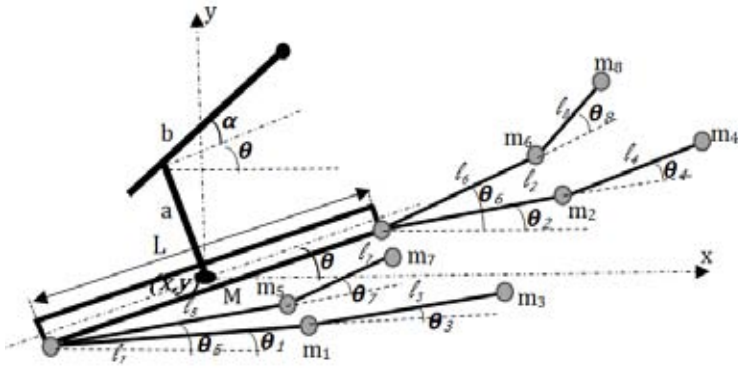


Figure 2. Physical model of the armed quadruped robot.

Lagrange equation (L) is based on the principle of total energy change. It is calculated by taking the difference between the total kinetic energy (T) of the system and the total potential energy (V). T and V equations are given in Eqns. (3) and (4). Descriptions of the parameters in the equation are given in nomenclature.

$$L = T - V \quad (2)$$

$$T = \frac{1}{2}M(\dot{x}^2 + \dot{y}^2) + \frac{1}{2}I\dot{\theta}^2 + \frac{1}{2}m_1(\dot{x}_1^2 + \dot{y}_1^2) + \frac{1}{2}m_2(\dot{x}_2^2 + \dot{y}_2^2) + \frac{1}{2}m_3(\dot{x}_3^2 + \dot{y}_3^2) + \frac{1}{2}m_4(\dot{x}_4^2 + \dot{y}_4^2) + \frac{1}{2}m_5(\dot{x}_5^2 + \dot{y}_5^2) + \frac{1}{2}m_6(\dot{x}_6^2 + \dot{y}_6^2) + \frac{1}{2}m_7(\dot{x}_7^2 + \dot{y}_7^2) + \frac{1}{2}m_8(\dot{x}_8^2 + \dot{y}_8^2) + \frac{1}{2}m_n(\dot{x}_n^2 + \dot{y}_n^2) \quad (3)$$

$$V = Mgy + m_1gy_1 + m_2gy_2 + m_3gy_3 + m_4gy_4 + m_5gy_5 + m_6gy_6 + m_7gy_7 + m_8gy_8 + m_ngy_n \quad (4)$$

In the Lagrange method, the robot body's position equations, gun barrel, and all legs for the equations of motion are given in Eqns. (5) - (22).

$$x_1 = x - \frac{1}{2}\cos\theta + l_1\cos\theta_1 \quad (5)$$

$$y_1 = y - \frac{1}{2}\sin\theta + l_1\sin\theta_1 \quad (6)$$

$$x_2 = x + \frac{1}{2}\cos\theta + l_2\cos\theta_2 \quad (7)$$

$$y_2 = y + \frac{1}{2}\sin\theta + l_2\sin\theta_2 \quad (8)$$

$$x_3 = x - \frac{1}{2}\cos\theta + l_1\cos\theta_1 + l_3\cos(\theta_1 + \theta_3) \quad (9)$$

$$y_3 = y - \frac{1}{2}\sin\theta + l_1\sin\theta_1 + l_3\sin(\theta_1 + \theta_3) \quad (10)$$

$$x_4 = x + \frac{1}{2}\cos\theta + l_2\cos\theta_2 + l_4\cos(\theta_2 + \theta_4) \quad (11)$$

$$y_4 = y + \frac{1}{2}\sin\theta + l_2\sin\theta_2 + l_4\sin(\theta_2 + \theta_4) \quad (12)$$

$$x_5 = x - \frac{1}{2}\cos\theta + l_5\cos\theta_5 \quad (13)$$

$$y_5 = y - \frac{1}{2}\sin\theta + l_5\sin\theta_5 \quad (14)$$

$$x_6 = x + \frac{1}{2}\cos\theta + l_6\cos\theta_6 \quad (15)$$

$$y_6 = y + \frac{1}{2}\sin\theta + l_6\sin\theta_6 \quad (16)$$

$$x_7 = x - \frac{1}{2}\cos\theta + l_5\cos\theta_5 + l_7\cos(\theta_5 + \theta_7) \quad (17)$$

$$y_7 = y - \frac{1}{2}\sin\theta + l_5\sin\theta_5 + l_7\sin(\theta_5 + \theta_7) \quad (18)$$

$$x_8 = x + \frac{1}{2}\cos\theta + l_6\cos\theta_6 + l_8\cos(\theta_6 + \theta_8) \quad (19)$$

$$y_8 = y + \frac{1}{2}\sin\theta + l_6\sin\theta_6 + l_8\sin(\theta_6 + \theta_8) \quad (20)$$

$$x_n = x - a\sin\theta + b\cos(\alpha + \theta) \quad (21)$$

$$y_n = y + a\cos\theta + b\sin(\alpha + \theta) \quad (22)$$

The expressions of velocity to be used in the measurement of kinetic energy were calculated by taking the time-based derivatives of the position expressions. Using these velocity equations, the general Lagrange function is obtained equations of motion (torque) were calculated and applied to the simulations.

Jacobian matrices are required to compute the effects of the reaction forces on the robot body that were applied from the ground to the robot's toes. The Jacobian matrix is the most accurate of the computational-based methods because it provides a transformation between velocities and kinematic structure in the work area¹⁴. Only the ground reaction forces x and y components are considered for planar motion. The necessary Jacobian matrix was obtained using the expression Eqn. (23). To find out the effect of the reaction force on the gun barrel during the shooting, the Jacobian matrix in Eqn. (24) is used.

$$[J] = \begin{bmatrix} \frac{\partial x_1}{\partial x} & \frac{\partial x_1}{\partial y} & \frac{\partial x_1}{\partial \theta} & \frac{\partial x_1}{\partial \theta_1} & \frac{\partial x_1}{\partial \theta_2} & \frac{\partial x_1}{\partial \theta_3} & \frac{\partial x_1}{\partial \theta_4} & \frac{\partial x_1}{\partial \theta_5} & \frac{\partial x_1}{\partial \theta_6} & \frac{\partial x_1}{\partial \theta_7} & \frac{\partial x_1}{\partial \theta_8} \\ \frac{\partial y_1}{\partial x} & \frac{\partial y_1}{\partial y} & \frac{\partial y_1}{\partial \theta} & \frac{\partial y_1}{\partial \theta_1} & \frac{\partial y_1}{\partial \theta_2} & \frac{\partial y_1}{\partial \theta_3} & \frac{\partial y_1}{\partial \theta_4} & \frac{\partial y_1}{\partial \theta_5} & \frac{\partial y_1}{\partial \theta_6} & \frac{\partial y_1}{\partial \theta_7} & \frac{\partial y_1}{\partial \theta_8} \end{bmatrix} \quad (23)$$

$$[J_n] = \begin{bmatrix} \frac{\partial x_n}{\partial x} & \frac{\partial x_n}{\partial y} & \frac{\partial x_n}{\partial \theta} & \frac{\partial x_n}{\partial \theta_1} & \frac{\partial x_n}{\partial \theta_2} & \frac{\partial x_n}{\partial \theta_3} & \frac{\partial x_n}{\partial \theta_4} & \frac{\partial x_n}{\partial \theta_5} & \frac{\partial x_n}{\partial \theta_6} & \frac{\partial x_n}{\partial \theta_7} & \frac{\partial x_n}{\partial \theta_8} \\ \frac{\partial y_n}{\partial x} & \frac{\partial y_n}{\partial y} & \frac{\partial y_n}{\partial \theta} & \frac{\partial y_n}{\partial \theta_1} & \frac{\partial y_n}{\partial \theta_2} & \frac{\partial y_n}{\partial \theta_3} & \frac{\partial y_n}{\partial \theta_4} & \frac{\partial y_n}{\partial \theta_5} & \frac{\partial y_n}{\partial \theta_6} & \frac{\partial y_n}{\partial \theta_7} & \frac{\partial y_n}{\partial \theta_8} \end{bmatrix} \quad (24)$$

The numerical values of the physical parameters of the robot are given in Table 1.

The robot legs are subjected to reaction forces from the ground in horizontal and vertical directions as they come into contact with the ground. The mechanical behaviour of

Table 1. Numerical values of the robots' physical parameters

Parameter	Value	Parameter	Value
M	12 kg	m_1, m_2, m_5, m_6	1.5 kg
l_g	0.8 m	m_3, m_4, m_7, m_8	0.5 kg
l_1, l_2, l_5, l_6	0.24 m	a	0.1 m
l_3, l_4, l_7, l_8	0.2 m	b	0.3 m
m_n	1 kg		

the structural material constituting the ground is modelled as shown in Fig. 3 with spring (k_{ground}) and damping (C_{ground}) elements. The physical model of the deformation formed by the contact of the foot with the ground is formed by spring and damping elements.

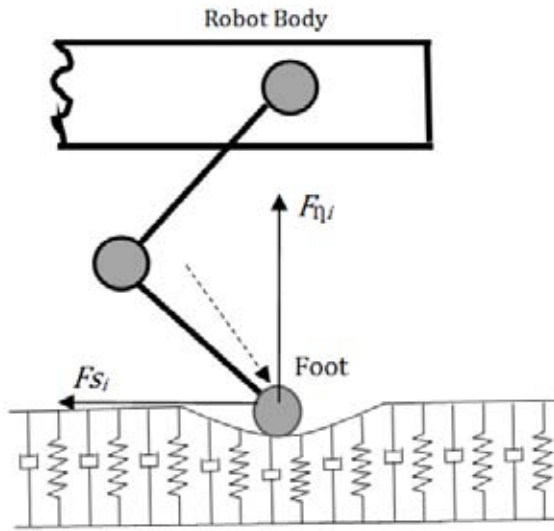


Figure 3. Physical modelling of the ground's mechanical behaviour.

Depending on the mechanical properties of the surface, the weight force exerted by the foot end on the ground surface or the impact force caused by it will cause the ground to collapse. The ground reaction force was calculated with the magnitude F_{η_i} in Eqn. (25), depending on its mechanical properties.

$$F_{\eta_i} = -k_{ground} y_i - c_{ground} \frac{dy_i}{dt} \quad (25)$$

When the robot feet come into contact with the ground, they are also subjected to surface friction forces in the horizontal direction. The ground reaction force that may occur during the contact of a moving leg with the ground is shown in Fig. 3 as F_{s_i} . These frictional forces are formed in the x-direction parallel to the surface. The surface dry friction coefficient is defined as μ parameter. The parameters to which the frictional forces (F_{s_i}) of each leg are connected are respectively; The F_{η_i} force perpendicular to the surface is the viscous damping coefficient (C_s) and the horizontal velocities of the feet on the surface. Based on these parameters, the frictional forces are calculated as in Eqn. (26).

$$F_{s_i} = -\mu F_{\eta_i} \text{sign} \left(\frac{dx_i}{dt} \right) - C_s \frac{dx_i}{dt} \quad (26)$$

By means of the Jacobian matrix (J) in Eqn. (23), the reaction torques (τ) caused by these reaction forces acting on each leg in the quadruped robot joints were calculated as in Eqn. (27).

$$\tau_i = J^T \begin{bmatrix} F_{s_i} \\ F_{\eta_i} \end{bmatrix} \quad (27)$$

3. WALKING PATTERN OF THE QUADRUPED ROBOT

The reasons for the wide use of PID control are simple structure, robustness, and easy application. The optimal parameters of PID control have a very important effect on the system where the control is applied¹⁵. The control signal according to the PID control method can be calculated as in Eqn. (28).

$$u(t) = K_p e(t) + K_d \frac{d e(t)}{dt} + K_i \int_0^t e(t) dt \quad (28)$$

here $e(t)$ refers to the error value. Proportional gain coefficient $K_p = 500$, the derivative gain coefficient $K_d = 50$, the integral gain coefficient $K_i = 0.1$ was found by the trial-and-error technique.

While the robot is walking, it is only intended to keep the body at a certain height. As a result, the reference coordinates for moving the legs were specified and, following these references, it was allowed to perform the walking. Afterward, the PID control method was used for the robot leg joints to track the reference joint angles for the selected walking pattern.

In this study, the trot walking sequence¹⁶ shown in Fig. 4 was used for simulations. The oscillations in the robot body resulting from this walking sequence are reflected as disruptive effects on the stabilisation of the gun barrel.

One leg tracks the curve route in the x-y plane during the robot's walk as shown in Fig. 5. Each step is made up of air and ground phases. The legs carry out in the air sinusoidal movements. In the stance phase, the leg is in constant contact with the floor and the foot is moved parallel to the ground directly. Thus, the body of the robot is held parallel to the ground by the leg in the stance phase. The walking has two half periods. The robot has two crossed legs in the air in this walking pattern and the other two legs touch the ground every half-period.

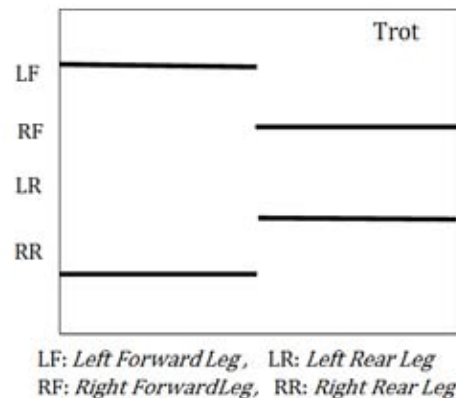


Figure 4. "Trot" walking of the quadruped robot.

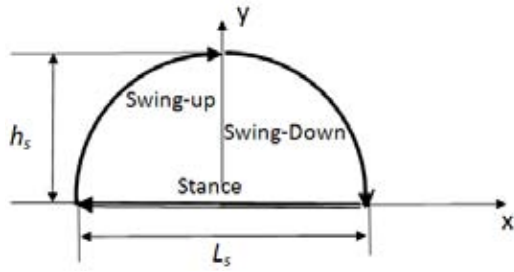


Figure 5. Swing and stance phases of the robot leg.

4. THE GUN BARREL STABILISATION WITH SLIDING MODE CONTROLLER

The SMC method gives a steady performance, simple designing, and a robust control¹⁷. The sliding-mode control design has a two-stage process. These stages are respectively; determining a sliding surface and defining a control rule for achieving the defined sliding surface. The control rule forces the dynamics of the system to reach the sliding surface. When the system dynamics reach the sliding surface, it is forced to keep on it. In this case, sliding mode occurs. In sliding control, the system is insensitive to parameter uncertainty and external disturbances¹⁸. Chattering in applications for sliding mode control is caused by oscillations around the balance point. The system wants to reach and it exposes the system’s unmodified high-frequency dynamics. The SMC expression with a sign function can be written as in Eqn. (29).

$$U = -K_{smc} \text{Sign}(s) \tag{29}$$

Here, S is given in Eqn. (30) and it is the sliding surface function depending on the error (e) and taken from the system and the derivative of the error (de). The K_{smc} coefficient in the expression is the largest value of the control output.

The error (e) here is the difference between the reference angle (β_{Target} = the gun barrel absolute angular position $\beta = (\alpha + \theta)$ relative to the x-axis) of the barrel and the absolute angle that the barrel makes relative to the x-axis ($e = \beta_{target} - \beta$). Here, the (θ) parameter is the swing angle of the robot body. The (α) parameter is the relative angle of barrel’s rotation to the body.

$$S = C_{smc} e + de \tag{30}$$

The sliding surface has a certain slope as seen in Fig. 6. This slope is indicated by the coefficient C_{smc} in Eqn. (30).

Control signals chattering has negative system effects. The SMC expression using a saturation function can be written as in Eqn. (31) to reduce the chattering problem.

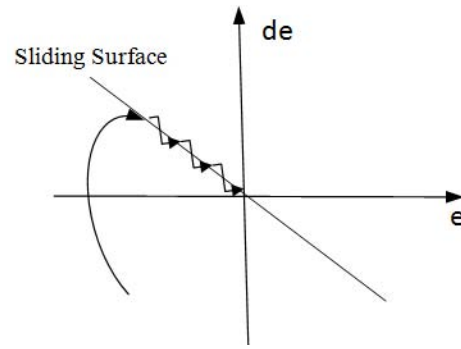


Figure 6. Sliding surface.

$$U = -K_{smc} \text{sat}\left(\frac{s}{\phi}\right) \tag{31}$$

Here ϕ is the boundary layer thickness. Accordingly, the saturation function can be calculated as in Eqn. (32).

$$\text{Sat}\left(\frac{s}{\phi}\right) = \begin{cases} 1 & \left(\frac{s}{\phi}\right) > 1 \\ -1 & \left(\frac{s}{\phi}\right) < -1 \\ \left(\frac{s}{\phi}\right) & -1 < \left(\frac{s}{\phi}\right) < 1 \end{cases} \tag{32}$$

5. SIMULATION RESULTS

5.1 Trot Walking Simulation of the Quadruped Robot

The trot walking of the robot is simulated in MATLAB. Fig. 7 shows an image taken from different stages of walking movement in the simulation. The robot proceeds a 4 m path at the end of a 7 s walking simulation.

The angular displacement of the robot body’s center around the axis perpendicular to the plane and linear displacements in the horizontal and vertical axis during the simulation are shown in Fig. 8. The vertical displacement is 3-4 cm in the first moments of the walk and the rolling amplitude is 2-3 cm. Oscillations appear on linear and angular position graphs. The cause of the oscillation in the vertical linear position (y-axis); is aimed to keep the body at a certain height.

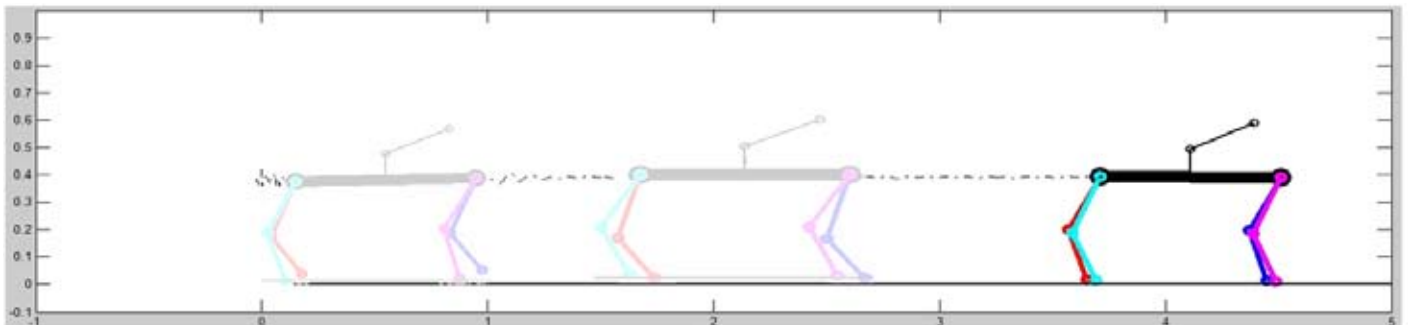


Figure 7. Trot walking simulation of the quadruped robot.

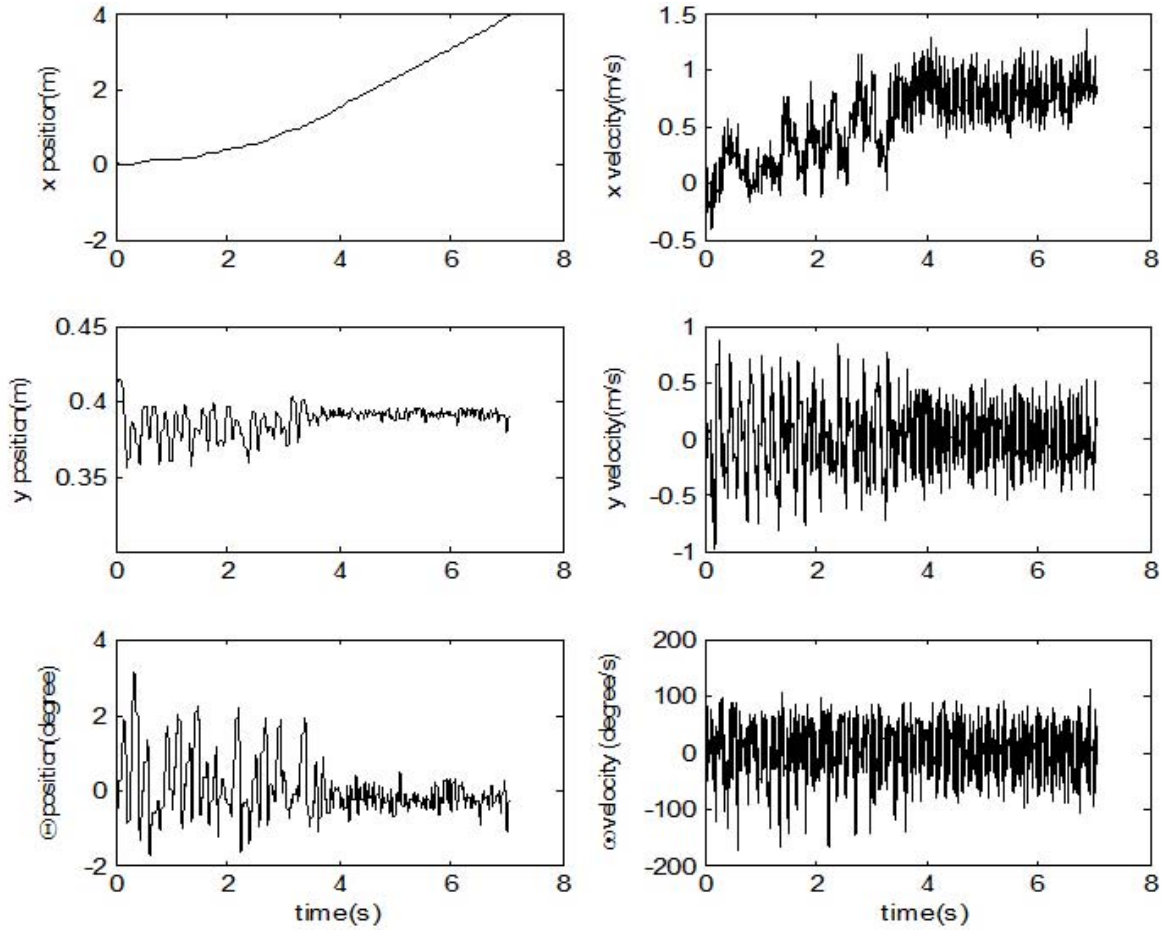


Figure 8. Graphics of position and velocity from the trot walking simulation.

5.2 Simulation of Barrel Stabilisation

While the robot is trot walking, the barrel angle of the gun turret mounted on the robot is aimed to be held in the targeted position in this analysis. The sliding-mode control system is used for this purpose. The control coefficients were obtained as $K_{smc} = 50$, $C_{smc} = 63$, $\varphi = 0.6$ with trial-and-error technique.

To determine the success of the sliding mode control method, the gun barrel should be kept in the reference position while walking the robot. For this, the reference angle is set at 12° . In the simulations, the gun barrel start angle was accepted as 0° .

Accordingly, the control and system responses of sliding-

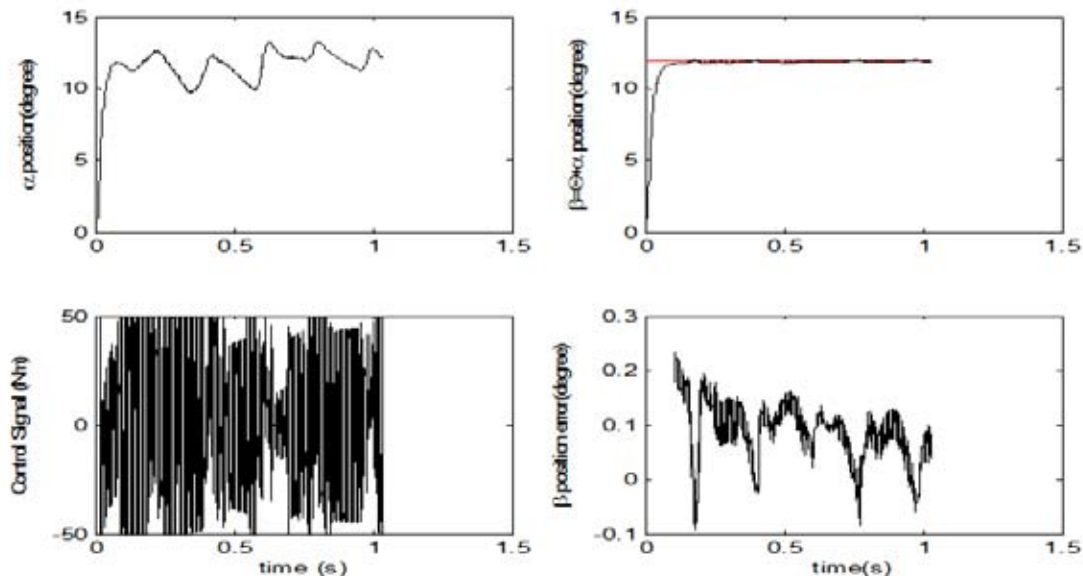


Figure 9. System responses of the gun barrel in simulation for 12° .

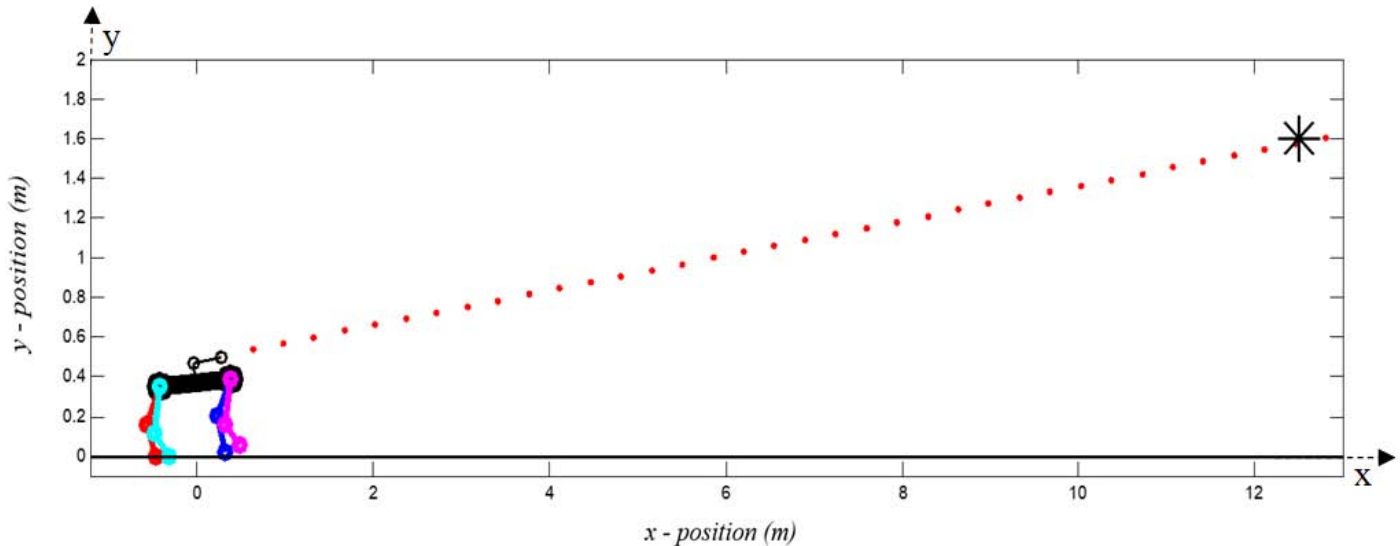


Figure 10. Shooting simulation diagram.

mode are presented graphically in Fig. 9. Because of the body movements, the gun barrel's relative angle α was seen to be oscillating. The sliding-mode controller has been able to successfully maintain the gun barrel absolute angular position $\beta=(\alpha+\theta)$ relative to the x-axis, at a target angle with very small errors and oscillating responses. The gun barrel's angular error was obtained at a maximum of 0.24° .

5.3 Simulation of Shooting Fixed Target

In this study, simulations were performed to shots aimed at fixed targets placed in randomly selected coordinates and evaluated the success of these shots. The shots were made under disruptive effects while the robot was walking and the gun barrel was controlled by the sliding mode control method. The target hitting simulation diagram is shown in Fig. 10.

The fixed targets' coordinates for the shooting simulations were determined randomly between 5-15 m in the horizontal axis and 0.5-2 m in the vertical axis. Throughout the simulation, β_{target} (reference angle) was auto-updated and simultaneously calculated, taking into account the variable position of the robot towards fixed targets while walking. The reference angle β_{target} is calculated as in Eqn. (33), depending on the position error of the weapon on the horizontal and the vertical axis.

$$\beta_{Target} = \tan\left(\frac{e_y}{e_x}\right) = \tan\left(\frac{y_{Target} - y_{gun}}{x_{Target} - x_{gun}}\right) \quad (33)$$

Table 2 shows the results of the shooting simulations for different 10 fixed targets. Coordinates of fixed targets and shooting error results are given in this table. Hit errors' highest values were seen as 0.14 m in 2nd, 9th and 10th shots. The smallest hit error value was 0.03 m in the 8th shot. The mean value of these errors is 0.095 m and the standard deviation is 0.043 m.

If the target distance is increased, it is thought that the projectile core will reach the target with a greater deviation because of gravity. To demonstrate the success of the gun barrel

Table 2. Shooting results

Target number	x_{target} (m)	y_{target} (m)	Error (m)
1	10.86	1.50	0.04
2	6.79	1.41	0.14
3	13.22	1.00	0.05
4	9.7	0.86	0.12
5	11.26	0.90	0.07
6	5.31	1.19	0.10
7	8.95	1.43	0.12
8	12.57	1.75	0.03
9	10.35	0.79	0.14
10	9.34	0.76	0.14

stabilisation, it was found appropriate to perform a simulation with short distance shots.

6. CONCLUSION

In this study, firstly, the quadruped robot's dynamical model is produced and the robot's trot walking results are presented with the designed PID controller. Secondly, the SMC controller was designed to stabilize the turret system on the robot. As the robot walked, shots were fired at fixed targets at randomly determined distances. The success of the SMC controller has been tested by shooting at fixed targets. Accordingly, the success of the shots directed to 10 different targets was examined and the numerical values were presented in a table. As a result of the shots made from these distances, it was revealed that a fixed target with a diameter of 14 cm could be hit with a very high success rate. With these successful results, it is clear that the weapon system placed on the quadruped robot can be used in practice for the defense industry. In line with the studies to be carried out in this area, it is thought that the literature contributes.

Future research should focus on the use of optimisation techniques to determine optimal control coefficients. In

addition, different control methods can be tried and compared. Finally, it is recommended that such systems are not used for any reason other than the purpose of deterrence.

REFERENCES

1. Neringa, M. Lessons from the past for weapons of the future. *Int. Comparative Jurisprudence*, 2016, **2**, 99-106. doi: 10.1016/j.icj.2017.01.002
2. Walsh, S. M.; Strano, M. S. & Stanton, S.C. Approaching robotics and autonomous systems as an integrated materials, energy, and control problem. *Robotic Sys. Autonomous Platforms*, 2019, 19-46.
3. Liu, Y., Mendiratta V. B., and Kishor S. T. Survivability analysis of telephone Access network. *In Proc. Of the 15th IEEE ISSRE'04*. Saint Malo, Bretagne, France, 2004. doi: 10.1109/ISSRE.2004.38
4. Kline, A.; Ahner, D. & Hill, R. The weapon-target assignment problem. *Comput. Operations Res.*, 2019, **105**, 226-236. doi: 10.1016/j.cor.2018.10.015
5. Lee, Y. W. Neural solution to the target intercept problems in a gun fire control system. *Neurocomputing*, 2007, **70**, 689-696. doi: 10.1016/j.neucom.2006.10.004
6. Öner, H. E.; Gürcan, M. B.; Başçuhadar, İ. & Balkan, T. Hydraulic simulator design. *In 2nd National Hydraulic Pneumatic Congress and Exhibition*, Izmir, Turkey, 2001, **2**, 239-252.
7. Gomes, M.; Dos, S. & Ferreira, A. M. Gun-turret modelling and control. *In 18th International Congress of Mechanical Engineering*, 2006, **18**, pp. 60-67. doi: 10.1016/j.procs.2019.06.054
8. Gao, Z.; Shi, Q.; Fukuda, T.; Li, C. & Huang, Q. An overview of biomimetic robots with animal behaviours. *Neurocomputing*, 2019, **332**, 339-350. doi: 10.1016/j.neucom.2018.12.071
9. Dini, N. & Majd, V. J. An MPC-based two-dimensional push recovery of a quadruped robot in trotting gait using its reduced virtual model. *Mech. Mach. Theory*, 2020, **146**, 103737. doi: 10.1016/j.mechmachtheory.2019.103737
10. Zhang, J.; Gao, F.; Han, X. & Chan, X. Trot gait design and CPG method for a quadruped robot. *J. Bionic Eng.*, 2014, **11**, 18-25. doi: 10.1016/S1672-6529(14)60016-0
11. Slotine, F. F. E. & Li, W. Applied nonlinear control. Prentice Hall, New Jersey, 1991, pp. 22-26.
12. Rahmat, M. S.; Hudha, K.; Idris, A. M. & Amer, N.H. Sliding mode control of target tracking system for two degrees of freedom gun turret model. *Adv. Military Technol.*, 2016, **11**(1), 390-397.
13. Beckers, T.; Kulić, D. & Hirche, S. Stable Gaussian process based tracking control of Euler-Lagrange systems. *Automatica*, 2019, **103**, 390-397. doi: 10.1016/j.automatica.2019.01.023
14. Filiposka, M. Z.; Djuric, A. M. & ElMaraghy, W. Complexity analysis for calculating the Jacobian matrix of 6DOF reconfigurable machines. *Procedia CIRP*, 2014, **17**, 218-223. doi: 10.1016/j.procir.2014.02.051
15. Feng, H.; Yin, C. B.; Weng, W. W.; Ma, W.; Zhou, J. J.; Jia, W. H. & Zhang, Z. Robotic excavator trajectory control using an improved GA based PID controller. *Mech. Sys. Signal Process.*, 2018, **105**, 153-168. doi: 10.1016/j.ymsp.2017.12.014
16. Cristina, P. S. & Vitor, M. Gait transition and modulation in a quadruped robot: A brainstem-like modulation approach. *In The 2009 IEEE/RSJ International Conference on Intelligent Robots and Systems*, 2011, **59**, 620-634. doi: 10.1016/j.robot.2011.05.003
17. Utkin, V. Variable structure systems with sliding modes. *IEEE Trans. Automatic Control*, 1977, **22**(2), 212-222. doi: 10.1109/TAC.1977.1101446
18. Edwards, C. & Spurgeon, S.K. Sliding mode control: Theory and applications. London: Taylor and Francis, 1998, pp. 108-118.

DECLARATION

Funding: No funding source for this research.

Conflict of Interest: No conflict of interest.

ACKNOWLEDGMENT

This study was carried out within the scope of a doctoral thesis named "Four-Legged Hunter Robot", conducted by Doç. Dr Oğuz Yakut, Department of Mechatronics Engineering at Firat University.

CONTRIBUTORS

Mr Ahmet Burak Tatar graduated in Mechatronics Engineering from Firat University, Turkey in 2012. He received a Master's in Mechatronics Engineering from Firat University, in 2015. Presently working as a research assistant in the Department of Mechatronics Engineering, at Firat University. His area of research includes Robotics, Machine Theory and Mechatronics. Contribution in the current study is mathematical modelling of the system.

Dr Alper Kadir Tanyıldızı graduated in Mechanical engineering from Yeditepe University, Turkey in 2007. He received a Master's in Mechanical Engineering from Firat University, Turkey, in 2011 and PhD in Mechatronics. Presently working as a Research Assistant in the Department of Mechatronics Engineering, at Firat University, in Elazığ-Turkey. His area of research includes Robotics, Machine Theory and Mechatronics. His contribution in the current study is simulating the system.

Dr Oğuz Yakut received the BAs., MS, and PhD in Mechanical Engineering from Firat University respectively in 1998, 2001, and 2007. Presently working as an Associate Professor at the Mechatronics Engineering Department. His research interests include artificial intelligence, robotics, and vibration control. His area of research includes robotics, machine theory and mechatronics. Contribution in the current study is design and control algorithms of the system. All authors are responsible for whole of the article.